

Use of small beams to obtain design parameters of fibre reinforced concrete

G. Giaccio ^a, J.M. Tobes ^b, R. Zerbino ^{b,*}

^a CIC-LEMIT, Faculty of Engineering, La Plata University, Argentina

^b CONICET, Faculty of Engineering, La Plata University, LEMIT, 52 el121 y 122, 1900 La Plata, Argentina

Received 2 May 2006; received in revised form 15 May 2007; accepted 12 October 2007

Available online 23 October 2007

Abstract

In 2002, the final recommendation for the bending test of steel fibre reinforced concrete was presented by the RILEM TC162-TDF Committee. The test is performed on notched beams of 150 × 150 mm cross section with central point loading and makes possible to obtain representative parameters of the post-peak behaviour, such as the equivalent and the residual strengths. This paper analyses the possibilities of application of small beams for the characterization of FRC following the general guidelines of the mentioned recommendation. The use of smaller beams may simplify the test and can be particularly justified in FRC for low height structural elements, considering the effects of fibre orientation. Beams of different sizes cast with concretes incorporating different type and contents of steel fibres were tested using a closed-loop testing machine; both deflections and the crack mouth opening displacements were recorded. It was found that the post-peak parameters of FRC can be obtained using beams of smaller size when the fibre length and aggregate size are compatible with the dimension of the mould.

© 2007 Elsevier Ltd. All rights reserved.

Keywords: Steel fibres; Fibre reinforced concrete; Equivalent strength; Residual strength; Specimen geometry

1. Introduction

Several methods have been applied to evaluate fibre reinforced concrete (FRC), the more frequently used being the flexural tests [1–6]. It has been widely recognised that a criterion based only on strength is not enough for FRC characterization, and that it is necessary to consider the post-peak behaviour and the gains in toughness. In 2002, the final recommendation for the bending test for steel fibre reinforced concrete was presented by the RILEM TC162-TDF Committee, which improves several aspects of other standards [7]. From the load–deflection curve equivalent flexural tensile strength and residual flexural tensile strength are obtained. These concepts of equivalent and residual strength have been applied to the analysis of

FRC under direct tension or shear [8,9]. The equivalent flexural strength can be directly applied to structural design [10].

The test is performed on notched beams (150 × 150 mm cross section) using central point loading. One of the greater advantages of this configuration is that it guarantees the stability throughout the test even for FRC with low contents of fibres or for plain concrete. Unlike unnotched specimens, the crack is located very close to the notch plane and the nonlinear deformations are absent in the rest of specimen, therefore, all the dissipated energy can be attributed to crack propagation. Another advantage of notched specimens is the possibility of characterising toughness in terms of CMOD (crack mouth opening displacement), which simplifies the test significantly avoiding the use of the frame [2]. The results are presented in terms of stresses being easier for design, an objective definition of first crack is adopted and the possible contribution of plain

* Corresponding author. Tel.: +54 221 4831144; fax: +54 221 4250471.
E-mail address: zerbino@ing.unlp.edu.ar (R. Zerbino).

concrete is discarded. The greatest limitation is the requirement of a closed-loop testing system, more expensive than the traditional equipment.

The RILEM TC162-TDF recommendation is supported by an extensive program developed between several research centres that studied the variability of the method, the approach to deflections from the use of the CMOD, as well as the distribution of fibres in the sections of specimens [11–13]. The effect of the change in the beams width was also analysed, concluding that if a standard specimen of 150 mm height, 500 mm span, and notch depth 25 mm is used, neither the average values nor the variability of parameters of toughness are modified [14]. When beams with different height (span and notch depth/beam height ratio were kept constant) were analysed, it was found that as height decreases the variability of test results increases, fibre orientation increases, and the area below the load–deflection curve decreases for the same deflection. The first crack stress and its variability also increase as the height decreases, but no significant effects have been noted on the post-peak parameters. A strong fibre orientation effect in thin elements has been verified by X-ray [15]. Finally, the effects of aggregate and fibre sizes were studied, concluding that the equivalent strengths and their variability were similar for aggregate maximum sizes up to 16 mm; in FRC with 32 mm maximum size aggregates, the equivalent strengths tend to increase as the fibres length increases [16].

The size of beams adopted in the RILEM recommendation makes possible the evaluation of concretes prepared with the most used aggregate and fibres sizes. However, keeping aggregates and fiber lengths compatible with the specimen size, the use of small beams will be attractive as they are easier to handle. Even more important than the practical purpose is that they can be more representative in order to evaluate FRC to be used in thin slabs, concrete sheets, reinforcements or other low height structural elements where a preferential orientation of the fibres may take place. This paper analyses the possibilities of application of small beams for the characterization of FRC.

2. The RILEM TC162-TDF bending test

The main objective of the RILEM TC162-TDF recommendation is to obtain dimensional parameters representative of the post-peak behaviour to be used in FRC structural design. Prisms with nominal size (width and

height) of 150 mm and 550 mm length are used. The aggregate maximum size is limited to 32 mm and the fibres length to 60 mm. A central point loading configuration is adopted; the specimen is rotated 90° around its longitudinal axis and notch of 25 ± 1 mm is performed at the mid-span. A closed-loop system controlling the rate of increase of deflection or CMOD must be used. The displacement transducer that measures the deflection shall be mounted on a rigid frame that is fixed to the test specimen at mid-height over the supports. The CMOD is also measured by a displacement transducer, the distance between the bottom of the specimen and the line of measurement must be 5 mm or less.

The load–deflection (δ) curve is used to calculate the post-peak parameters. Firstly, the first crack load (F_L , using an offset of 0.05 mm) is defined and after that the first crack stress ($f_{ct,L}$) and the first crack deflection (δ_L). Two equivalent flexural tensile strengths ($f_{eq,2}$ and $f_{eq,3}$) that represent the mean stress value up to a defined deformation at the post-peak are calculated. The established deflections for $f_{eq,2}$ and $f_{eq,3}$ are $\delta_2 = \delta_L + 0.65$ mm, and $\delta_3 = \delta_L + 2.65$ mm respectively. To consider the contribution of plain concrete a triangle F_L height and 0.3 mm base is discounted. In addition four residual flexural tensile stresses ($f_{R,i}$) representing the load capacity at different deflections or CMOD (implying a same rotation angle) are calculated. In this case the deflections considered are $\delta_{R,1} = 0.46$ mm or $CMOD_1 = 0.5$ mm, $\delta_{R,2} = 1.31$ mm or $CMOD_2 = 1.5$ mm, $\delta_{R,3} = 2.15$ mm or $CMOD_3 = 2.5$ mm y $\delta_{R,4} = 3.0$ mm or $CMOD_4 = 3.5$ mm. Greater details can be found in the RILEM recommendation [7]. In 2005 an European standard based on the mentioned recommendation has been published [17].

3. Test program

3.1. Test specimens and calculation criterion

Six groups of tests with different types of specimens and loading arrangements were selected in this study; the main characteristics are included in Table 1. In all cases the notch depth/height ratio remains constant. Group A represents the test configuration given in the recommendation. In groups A, B, C, D, and F the height/span length ratio remains constant and equal to 0.25, while in group E this relationship is 0.18. The effect of beam size can be analysed

Table 1
Groups of specimens

Group	Beam length (mm)	Beam height, h (mm)	Notch depth, a (mm)	Beam width, w (mm)	Span length, l (mm)	a/h	$(h-a)/l$	Rotation respect to casting direction
A	550	153	26	152	500	0.17	0.25	90°
B	450	103	17.5	103	350	0.17	0.25	90°
C	450	103	17.5	103	350	0.17	0.25	0°
D	430	103	17.5	75	350	0.17	0.25	90°
E	430	75	13	103	350	0.17	0.18	0°
F	550	152	26	75	500	0.17	0.25	0°

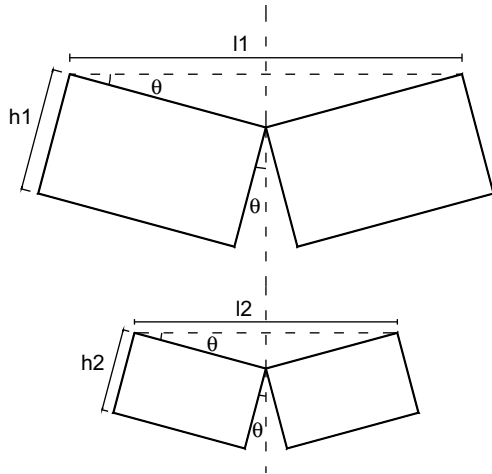


Fig. 1. Scheme of deflections and CMOD in the post-peak in beams with different heights.

comparing groups A and B, group B has typical dimensions adopted by other FRC standards, as for instance ASTM C 1018 [18]. Groups B and C compare the effect of rotation, meanwhile groups B and D analyse the influence of the specimen width. Considering groups A vs. F and C vs. D both the width and the orientation of the specimens are compared. Finally, groups D and E have different orientation and height/span ratio.

The equivalent and the residual flexural tensile strengths are calculated from the load–deflection or load–CMOD curves. Both of them change in accordance with the used type of beam (see Fig. 1). In the post-peak region, for a rotation angle θ , a beam with span length = l and height = h , has:

$$\text{deflection} = l/2 \cdot \theta \quad (1)$$

$$\text{CMOD} = h \cdot 2 \cdot \theta \quad (2)$$

then, if the l/h ratio remains constant, the deflection/CMOD is not modified.

In addition, in prisms with heights h_1 and h_2 , assuming $K = l/(2h)$:

$$\text{deflection}_2 = K \cdot h_2 \cdot \theta \quad (3)$$

$$\text{deflection}_1 = K \cdot h_1 \cdot \theta \quad (4)$$

and for a same rotation θ

$$\text{deflection}_1 = \text{deflection}_2 \cdot (h_1/h_2) \quad (5)$$

$$\text{CMOD}_1 = \text{CMOD}_2 \cdot (h_1/h_2) \quad (6)$$

Therefore, if the span/height and notch depth/height ratios remain constant, the deformation limits to calculate the equivalent and residual strengths must be corrected in accordance with the beam height. For instance in a 105 mm height prism, the displacements δ_2 and δ_3 should be:

$$\delta_2 = \delta_L + 0.65 \text{ h}/150 \text{ mm}, \quad \delta_2 = \delta_L + 0.455 \text{ mm} \quad (7)$$

$$\delta_3 = \delta_L + 2.65 \text{ h}/150 \text{ mm}, \quad \delta_3 = \delta_L + 1.855 \text{ mm} \quad (8)$$

In the same way the adopted offset for the definition of the first crack load and the deflections or CMOD used to calculate the residual strengths should be also corrected by the factor $h \text{ (mm)}/150 \text{ mm}$.

Another easier procedure to calculate the post-peak parameters with the small beams (with the same span/height ratio), is to multiply directly the deformation in the load–deflection (or CMOD) curves by the relationship $150 \text{ mm}/h \text{ (mm)}$, and then to calculate as it is indicated in the RILEM recommendation.

Although, due to size effect, small beams can present higher tensile strength they can be more representative in order to evaluate FRC to be used in thin structural elements.

3.2. Materials and concrete mixtures

Four FRC were prepared varying the type and content of hooked-ended collated steel fibres (F1 and F2, see Table 2). Concrete were prepared using water/cement ratio 0.40; natural siliceous sand, granitic crushed stone (19 mm maximum size), and a naphthalene-based superplasticizer. As it can be seen in Table 3, FRC with high, medium and low contents of F1 fibre were included. Slumps between 90 and 150 mm and Inverted Cone times between 7 and 13 s, were measured. In concretes C1-40 and C1-80 all groups of prisms were analysed, in concretes C1-20 and C2-40 only some of the groups were studied. Six prisms for each group plus four standard cylinders ($150 \times 300 \text{ mm}$) were cast. Specimens were filled and compacted by external vibration.

Table 2
Characteristics of the fibres

Steel fibers	F1	F2
Carbon content	High	Low
Tensile strength (MPa)	>2500	>1100
Maximum elongation (%)	>1.0	>0.8
Length (mm)	30	60
Aspect ratio	60	80

Table 3
Concretes

Concrete	C1-20	C1-40	C1-80	C2-40
Water/cement	0.40			
Ordinary Portland Cement (kg/m ³)	400			
Fine aggregate (kg/m ³)	900			
Coarse aggregate (kg/m ³)	900			
Superplasticizer (l/m ³)	2.5			
Fibre type	F1	F1	F1	F2
Content (kg/m ³)	20	40	80	40
Type of cast beams	A, B, D	A–F	A–F	A, B, E
Results on $150 \times 300 \text{ mm}$ cylinders				
Compressive strength (MPa)	37.4	56.0	59.7	53.6
Standard deviation	3.1	1.2	0.9	0.2
Modulus of elasticity (GPa)	32.9	39.3	36.6	35.7
Standard deviation	1.4	2.8	0.4	1.0

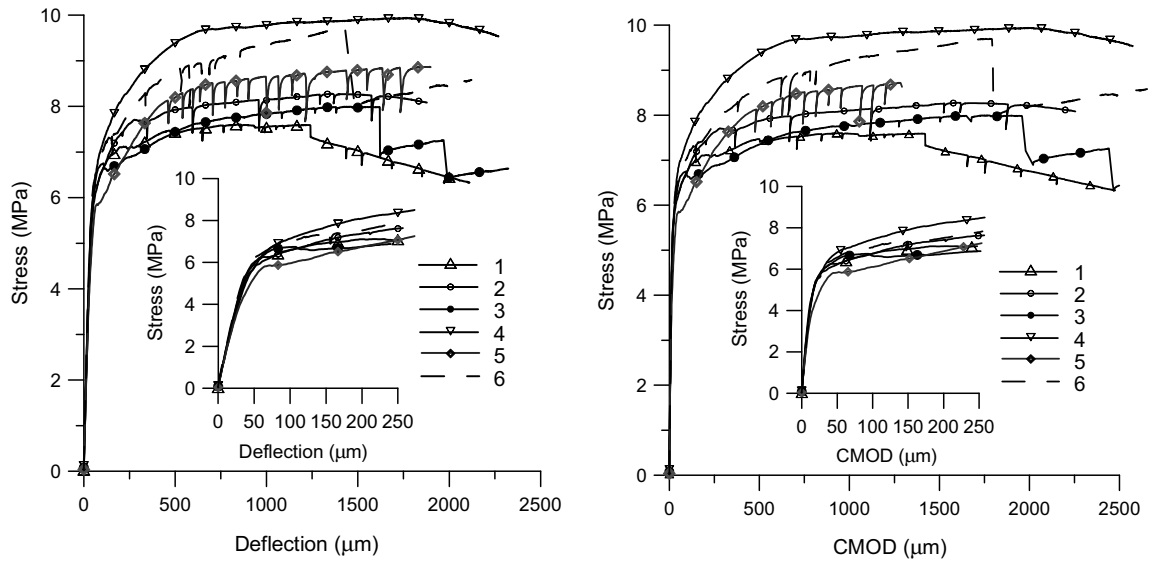


Fig. 2. Concrete C1-80: stress–deflection and stress–CMOD curves corresponding to each specimen of group A.

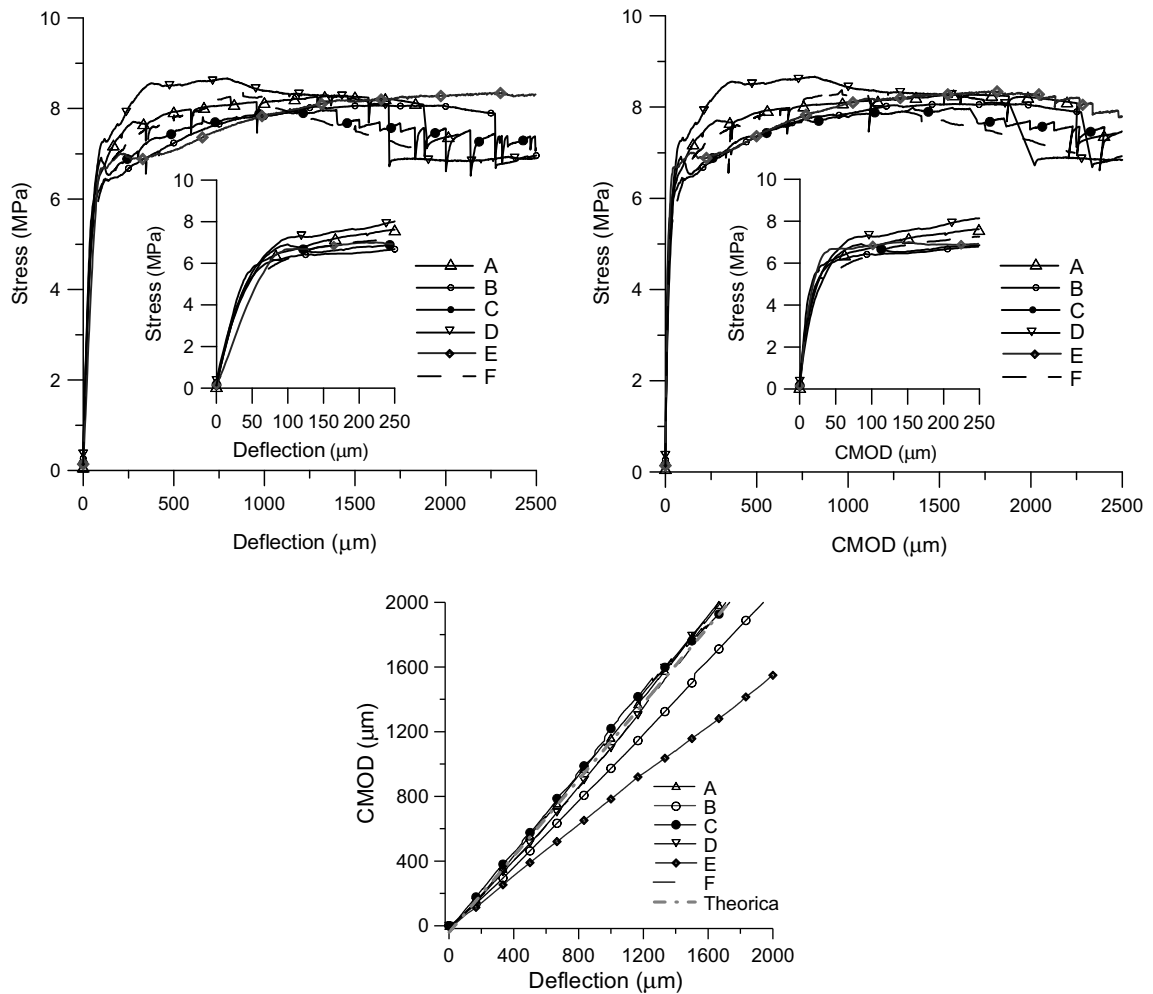


Fig. 3. Concrete C1-80: stress–deflection and stress–CMOD curves corresponding to a typical response of each group. Below: relationship between CMOD and deflection.

3.3. Experimental details

Tests were performed at 28 days. The notches were sawn one day before testing. In groups C, E and F the specimens were not rotated, applying the load on the casting surface.

Flexural tests were performed with an INSTRON closed-loop system using the deflection as a control signal at a rate of 0.20 mm/min. The LVDT was mounted between two rigid frames fixed at both sides of the test specimen, which can be adapted to different span lengths (500 or 350 mm). The CMOD was measured through a clip-gage fixed at 2 mm from the bottom of the beam.

The first crack load (F_L), equivalent (f_{eq}) and the residual (f_R) flexural tensile strengths were calculated from the load–deflection (δ) or load–CMOD curves, as indicated in the recommendation. In the smaller prisms (Groups B, C, D and E) the results were obtained from the corrected curves (deflections and CMOD were corrected applying Eqs. (5) and (6), respectively).

4. Results and discussion

Concrete C1-80 is a typical example of high fibre content, where a strengthening type post-peak behaviour and a less marked first-peak load are expected. Fig. 2 shows the stress–deflection and stress–CMOD curves of the six specimens of Group A. The observed variability can be accepted as characteristic of FRC. The initial portion of the curves (see inset) shows that after the first linear part there is not a decrease in loading capacity, then the first-crack load was obtained from the intersection between the curve and the parallel with an offset of 0.05 mm. It can be seen that the first crack points are very close. After a deflection near 40–50 μm the CMOD increases more than the deflection, that is in accordance with the theoretical relationship between CMOD and deflection indicated by the RILEM Recommendation ($\text{CMOD} = 1.18 * \delta - 0.0416 \text{ mm}$).

The stress–deflection and stress–CMOD curves of concretes C1-80, C1-40, C1-20 and C2-40 are given in

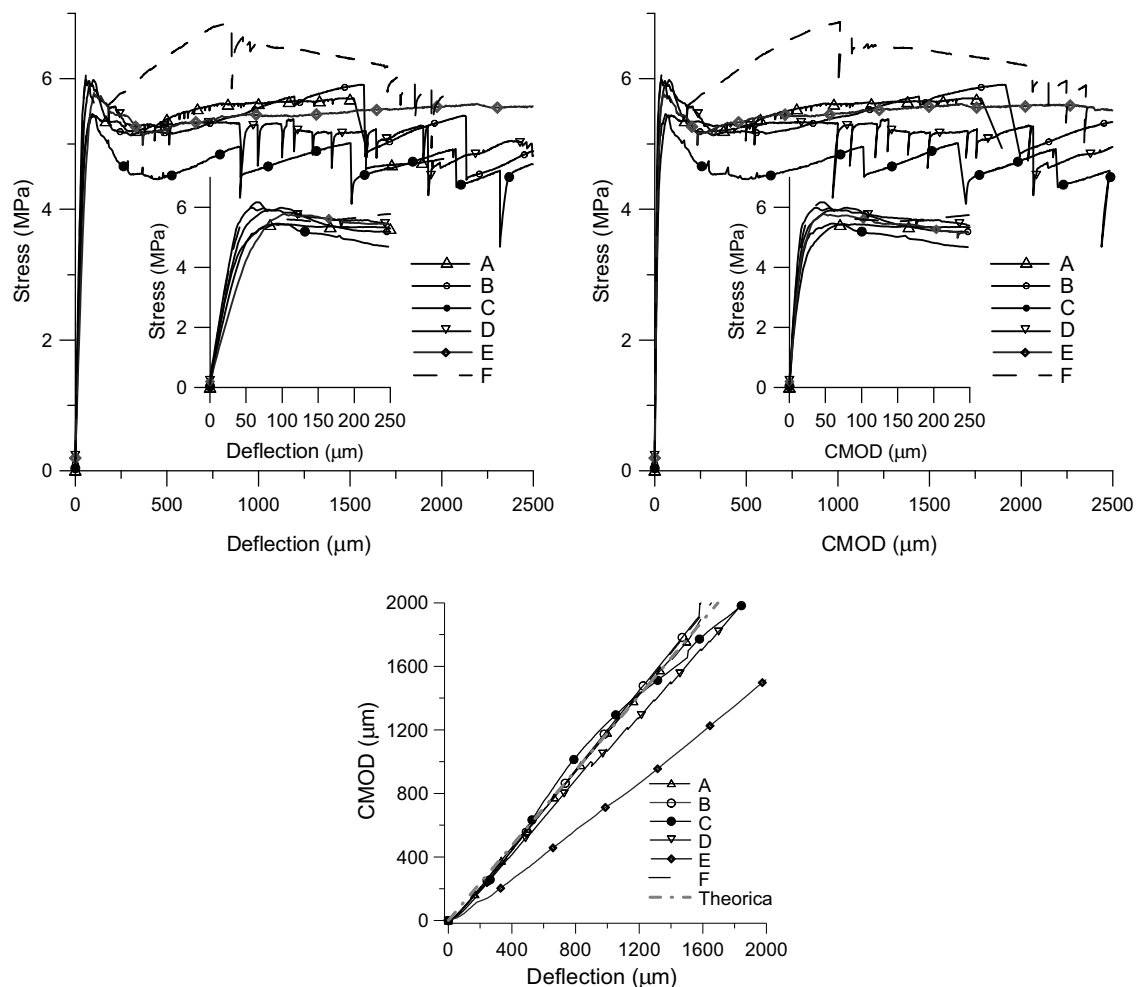


Fig. 4. Concrete C1-40: stress–deflection and stress–CMOD curves corresponding to a typical response of each group. Below: relationship between CMOD and deflection.

Figs 3–6. The curves nearer to the average behaviour of each group are represented. As it was indicated in Section 3.1, the deformations (deflections or CMOD) were corrected by a factor 150 mm/h mm in order to compare the bending behaviour of beams with different height.

Fig. 3 shows the stress–deflection and stress–CMOD curves of C1-80. The enlargement of the initial part up to 250 μm and the theoretical and experimental deflection vs. CMOD curves are also included. It is evident that the different Groups conform a coherent set. In group E, where a different height/span ratio was used, the relationship between deflection and CMOD changes.

Concrete C1-40 is a FRC with a well defined first peak and a post-peak behaviour without strengthening. Fig. 4 shows representative stress–deflection and stress–CMOD curves of each group. Again it can be seen that the curves obtained with the different test configurations fit a coherent set. Unlike C1-80, an elasto-plastic behaviour is now observed. It is also verified the relationship between CMOD and deflection, with the exception of Group E.

Concrete C1-20 constitutes a typical example of very low contents of fibres where a post-peak behaviour with a constant decrease in load capacity after first crack must

be expected. Fig. 5 shows that the stress–deflection and stress–CMOD curves of the studied groups (A, B and D) are very close. The initial part of the curves shows that the first crack deformations are smaller than those measured in C1-80 and C1-40. This fact can be attributed to the lower crack control capacity of the reinforcement.

The fibre length is limited to 60 mm in the RILEM Recommendation, then the fibre length/minimum dimension of specimen ratio is 0.4. Concrete C2-40 incorporates 60 mm length fibres (F2) with aspect ratio higher than F1, for this reason a preferential orientation as the mould dimensions decrease may take place. Using this type and content of fibres, an elasto-plastic behaviour with a greater strengthening than those observed in C1-40 was expected, even though F2 are low carbon steel fibres. Fig. 6 shows typical stress–deflection and stress–CMOD curves obtained from groups A, B and E. While the initial part of the curves is similar, the post-peak load capacity increases as the beams height decreases; this fact is attributed to a stronger fibre orientation.

The mean results and the standard deviation (SD) from the different Groups of concrete C1-80 are presented in Table 4. It includes the dimensions of the beams, the dis-

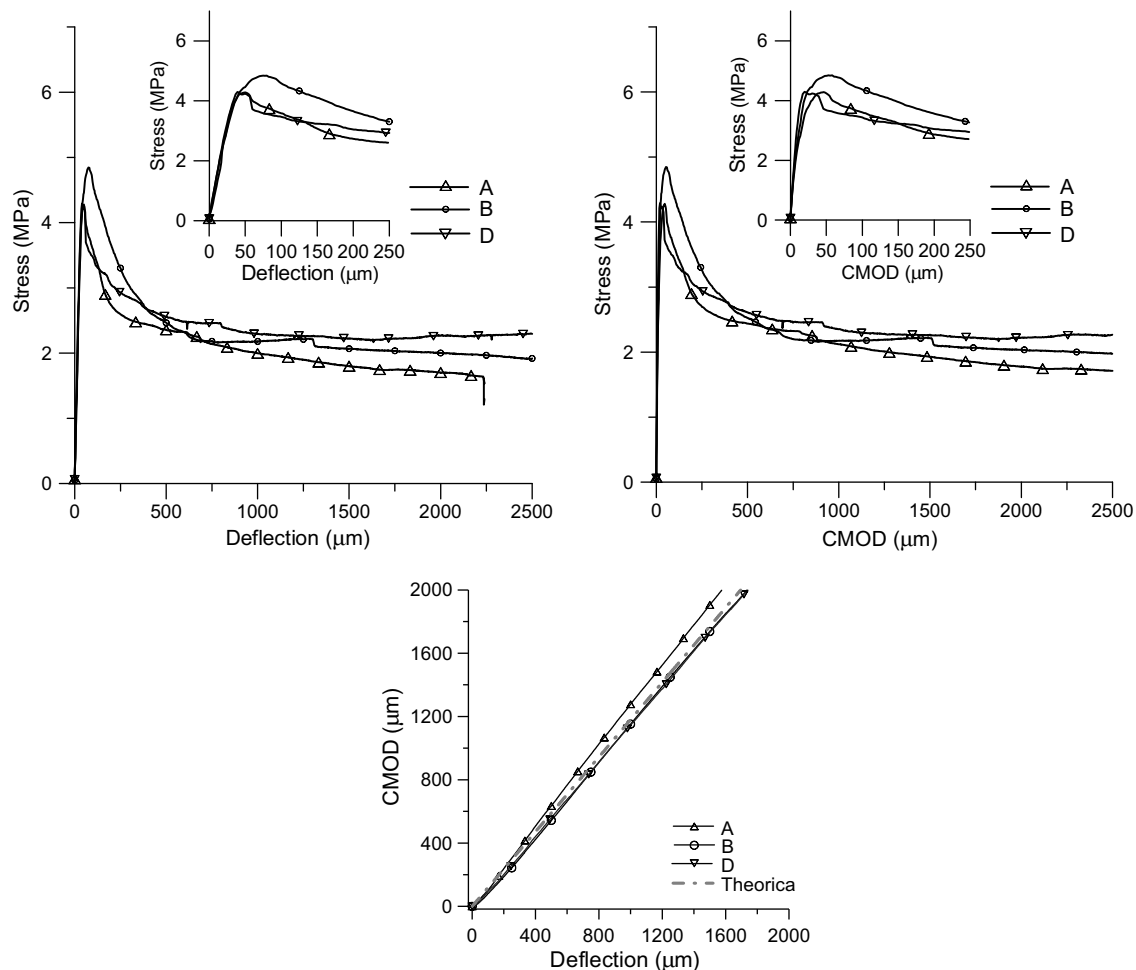


Fig. 5. Concrete C1-20: stress–deflection and stress–CMOD curves corresponding to a typical response of each group. Below: relationship between CMOD and deflection.

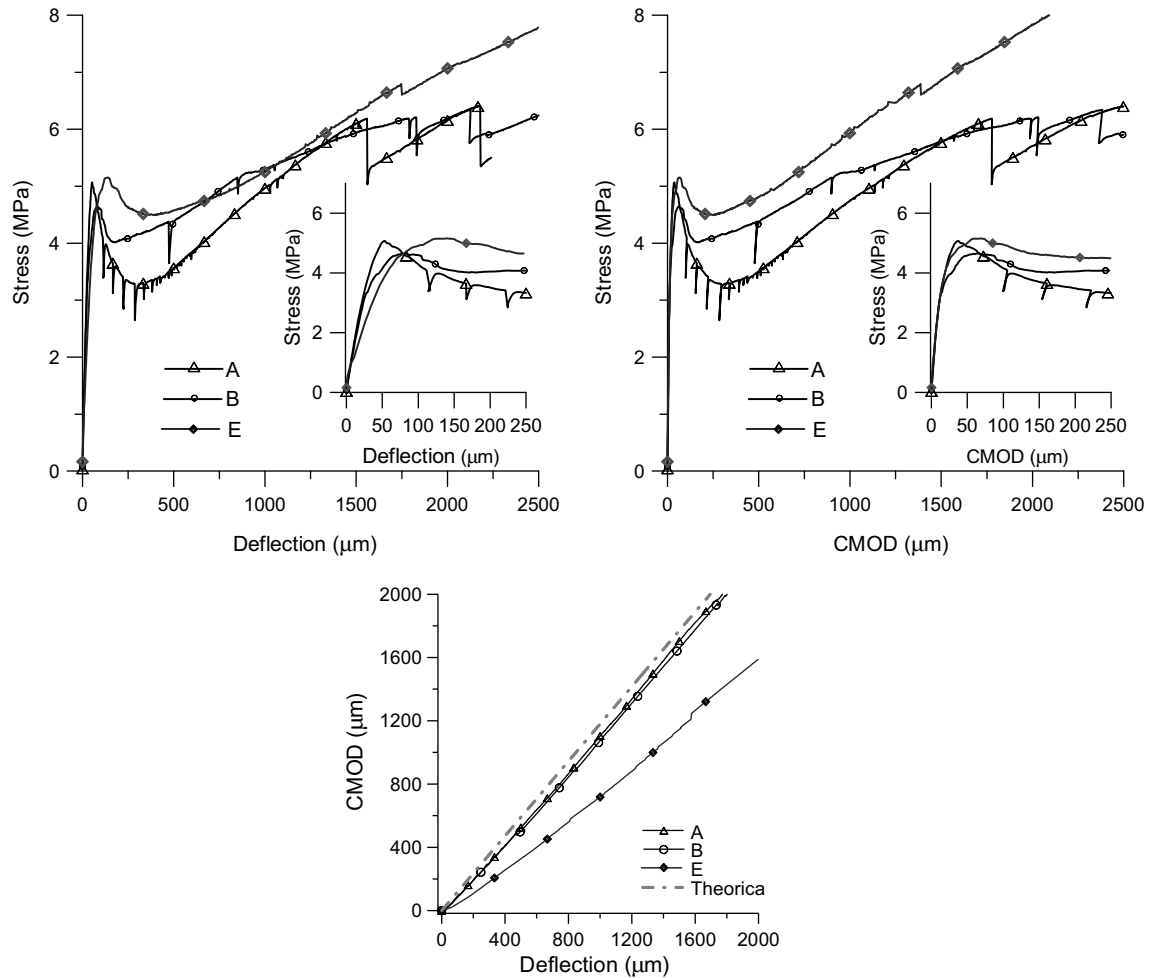


Fig. 6. Concrete C2-40: stress–deflection and stress–CMOD curves corresponding to a typical response of each group. Below: relationship between CMOD and deflection.

placements (δ_L and $CMOD_L$) and stress ($f_{ct,L}$) corresponding to first crack load, and the maximum stress ($f_{ct,R}$, calculated from the maximum load obtained along the entire test). As post-peak parameters the equivalent strengths f_{eq2} and f_{eq3} and the residual strengths $f_{R,1-CMOD}$, $f_{R,2-CMOD}$, $f_{R,3-CMOD}$, and $f_{R,1-\delta}$, $f_{R,2-\delta}$, $f_{R,3-\delta}$ and $f_{R,4-\delta}$ are included. In the same way the results corresponding to C1-40, C1-20 and C2-40 are given in Tables 5–7.

Experimental data was statistically analysed using the software SYSTAT (SYSTAT, Inc., Evanston, Ill., USA, 1990) version 5.0. First, an analysis of variance (ANOVA) was performed. When significant differences were detected, a Dunnett test was applied to know which of the median were different from control. The significance level (α) employed in all cases was equal to 0.10. This relative high value was chosen in order to minimise the probability of accepting that the measured property does not differ from control (group A) when it does.

Some differences were detected in stress ($f_{ct,L}$) corresponding to first crack load, and the maximum stress ($f_{ct,R}$) of groups B, D, E and F, specially for low or medium fibre contents. There were also found differences in the

first crack displacements (δ_L or $CMOD_L$). However, it must be emphasised that the post-peak parameters calculated for all Groups show no significant differences ($p > 0.10$) when compared with group A.

It was verified that the test method is robust showing variability equal or lower than other standards for bending test of FRC. From the results of Tables 4–7 it can be seen that, as expected, the variability tends to be higher in the post-peak parameters than in $f_{ct,R}$ or in $f_{ct,L}$.

Comparing the mean values of the different groups, some effects can be inferred. Usually the first crack deflection (δ_L) and $CMOD_L$ are similar for all groups, with the exception of group E, where a different height/span ratio was used.

There are differences in the first crack stress between small beams and standard beams that can be justified by fracture mechanics. However, it must be noted that concrete C1-80, prepared with high content of fibres no differences were observed.

The slight tendency to variation of the mean values between groups B and C (same specimen but different orientation) can be attributed to a better termination and

Table 4
Concrete C1-80

Group		<i>h</i> (mm)	<i>a</i> (mm)	<i>w</i> (mm)	δ_L (μ m)	CMOD _L (μ m)	$f_{ict,L}$ (MPa)	$f_{ict,R}$ (MPa)	f_{eq2} (MPa)	f_{eq3} (MPa)	$f_{R-\delta}$ (MPa)	$f_{R2-\delta}$ (MPa)	$f_{R3-\delta}$ (MPa)	$f_{R4-\delta}$ (MPa)	$f_{R,1-CMOD}$ (MPa)	$f_{R,2-CMOD}$ (MPa)	$f_{R,3-CMOD}$ (MPa)
A	Mean	154	27	152	96	78	6.6	8.7	9.2	8.3	8.1	8.7	8.0	6.9	8.1	8.5	7.0
	SD	1	2	2	4	6	0.4	0.9	0.9	1.0	0.8	0.9	1.2	0.8	0.8	1.0	1.4
B	Mean	101	18	101	105	84	7.2	9.1	9.5	8.6	8.3	9.0	8.3	7.2	8.3	9.0	8.0
	SD	1	1	2	4	7	0.7	0.9	1.1	0.8	1.0	0.8	0.7	0.4	0.9	0.8	1.0
C	Mean	101	17	101	99	83	6.5	8.6	8.9	8.2	7.8	8.4	7.8	7.7	7.8	8.4	7.9
	SD	1	1	1	7	6	0.3	0.6	0.6	0.6	0.6	0.7	0.8	0.4	0.6	0.7	0.7
D	Mean	104	16	75	111*	90	7.2	9.1	9.8	8.4	8.4	8.7	7.6	6.8	8.5	8.5	7.6
	SD	1	1	1	18	23	0.7	1.0	1.2	1.0	1.0	1.1	1.0	1.5	1.1	0.9	1.1
E	Mean	75	14	104	136*	69	6.4	8.4	8.3	8.0	6.9	8.1	8.0	7.5	7.3	8.3	7.5
	SD	2	3	1	14	8	0.5	0.8	1.0	0.8	0.7	0.8	0.8	1.0	0.9	0.8	1.0
F	Mean	153	23	77	96	81	6.3	8.2	8.7	7.5	7.7	7.7	6.3	–	7.7	7.8	6.5
	SD	2	2	4	4	3	0.4	1.0	0.8	1.2	0.7	1.3	1.6	–	0.7	1.2	1.3

* Mean values that differ from control (group A) with a significance level of 10% ($\alpha = 0.10$).

Table 5
Concrete C1-40

Group		<i>h</i> (mm)	<i>a</i> (mm)	<i>w</i> (mm)	δ_L (μ m)	CMOD _L (μ m)	$f_{ict,L}$ (MPa)	$f_{ict,R}$ (MPa)	f_{eq2} (MPa)	f_{eq3} (MPa)	$f_{R1-\delta}$ (MPa)	$f_{R2-\delta}$ (MPa)	$f_{R3-\delta}$ (MPa)	$f_{R4-\delta}$ (MPa)	$f_{R,1-CMOD}$ (MPa)	$f_{R,2-CMOD}$ (MPa)	$f_{R,3-CMOD}$ (MPa)
A	Mean	155	26	149	80	69	5.2	5.5	5.5	4.8	5.0	5.2	4.8	4.1	4.9	5.2	4.1
	SD	1	1	1	16	16	0.4	0.5	0.7	0.6	0.7	0.6	0.7	0.6	0.5	0.6	0.7
B	Mean	102	19	100	89	75	5.8*	5.8	5.4	4.9	4.9	5.3	4.6	4.4	4.8	5.2	4.7
	SD	1	3	2	15	27	0.2	0.2	0.6	0.5	0.7	0.6	0.2	0.3	0.6	0.6	0.4
C	Mean	99	16	102	89	66	5.5	5.6	5.1	4.7	4.7	4.8	4.5	4.1	4.4	4.7	4.4
	SD	3	1	2	15	16	0.4	0.3	0.4	0.5	0.6	0.5	0.6	0.7	0.3	0.6	0.7
D	Mean	104	17	76	61	38*	6.0*	6.2*	5.1	5.1	5.0	5.3	5.2	4.6	4.8	5.4	5.2
	SD	1	1	1	6	5	0.2	0.5	1.4	1.1	1.1	1.0	1.0	0.9	1.2	1.0	1.1
E	Mean	76	13	104	124*	66	5.7	5.9	6.0	5.3	4.9	5.0	5.3	4.9	5.1	5.2	4.9
	SD	1	1	1	27	18	0.3	0.4	0.7	0.7	0.5	0.7	0.7	0.8	0.6	0.7	0.8
F	Mean	151	23	75	70	51	5.3	6.1*	5.8	5.3	5.0	5.5	5.4	4.7	5.4	5.5	4.7
	SD	2	4	2	10	13	0.7	0.7	0.7	0.9	0.9	0.8	1.1	1.1	0.7	1.1	1.1

* Mean values that differ from control (group A) with a significance level of 10% ($\alpha = 0.10$).

Table 6
Concrete C1-20

Group		h (mm)	a (mm)	w (mm)	δ_L (μm)	CMOD _L (μm)	$f_{\text{ict,L}}$ (MPa)	$f_{\text{ict,R}}$ (MPa)	f_{eq2} (MPa)	f_{eq3} (MPa)	$f_{\text{R1}-\delta}$ (MPa)	$f_{\text{R2}-\delta}$ (MPa)	$f_{\text{R3}-\delta}$ (MPa)	$f_{\text{R4}-\delta}$ (MPa)	$f_{\text{R,1-CMOD}}$ (MPa)	$f_{\text{R,2-CMOD}}$ (MPa)	$f_{\text{R,3-CMOD}}$ (MPa)
A	Mean	155	25	154	50	46	4.0	4.0	2.4	1.9	2.3	1.9	1.7	1.3	2.4	2.0	1.7
	SD	1	1	1	3.9	5.5	0.3	0.3	0.3	0.3	0.3	0.3	0.2	0.3	0.3	0.4	0.3
B	Mean	102	15	102	76*	58	4.8*	4.8*	2.8	2.1	2.5	2.0	1.8	1.6	2.5	2.0	1.8
	SD	1	1	2	4.9	7.0	0.2	0.2	0.5	0.4	0.4	0.3	0.3	0.3	0.4	0.3	0.3
D	Mean	104	16	78	57	40	4.7*	4.7*	2.7	2.2	2.5	2.2	2.1	1.7	2.5	2.2	2.0
	SD	1	1	1	9.9	12.0	0.2	0.2	0.4	0.5	0.4	0.5	0.5	0.7	0.4	0.5	0.5

* Mean values that differ from control (group A) with a significance level of 10% ($\alpha = 0.10$).

Table 7
Concrete C2-40

Group		h (mm)	a (mm)	w (mm)	δ_L (μm)	CMOD _L (μm)	$f_{\text{ict,L}}$ (MPa)	$f_{\text{ict,R}}$ (MPa)	f_{eq2} (MPa)	f_{eq3} (MPa)	$f_{\text{R1}-\delta}$ (MPa)	$f_{\text{R2}-\delta}$ (MPa)	$f_{\text{R3}-\delta}$ (MPa)	$f_{\text{R4}-\delta}$ (MPa)	$f_{\text{R,1-CMOD}}$ (MPa)	$f_{\text{R,2-CMOD}}$ (MPa)	$f_{\text{R,3-CMOD}}$ (MPa)
A	Mean	154	27	151	62	47	4.7	6.6	4.3	5.7	4.0	6.1	6.2	4.4	5.4	6.1	6.3
	SD	1	2	1	17	18	0.3	1.0	0.8	0.9	0.6	0.9	1.1	1.4	0.9	1.2	1.1
B	Mean	102	16	102	87*	69*	5.1	6.5	4.5	5.4	3.9	5.4	6.1	4.1	5.5	5.9	6.1
	SD	1	1	2	10	5	0.6	1.6	1.3	1.6	1.1	1.8	1.7	0.9	1.7	1.9	1.9
E	Mean	75	14	104	152*	77*	5.1	8.3*	5.8	6.2	4.9	6.4	7.6	4.7	5.7	6.7	7.8
	SD	<1	3	2	38	20	0.7	1.1	1.2	0.8	0.5	0.9	1.4	1.0	0.5	0.9	0.9

* Mean values that differ from control (Group A) with a significance level of 10% ($\alpha = 0.10$).

parallelism of the surfaces, as other studies indicate that there are no substantial differences in the fibre orientation between both planes [19]. The mentioned effect can justify the small differences in the stresses in groups A and F of C1-80 (changes in the orientation and reduction of the width of the beams), as previous studies demonstrated a reduced influence of the beam width on the test parameters [14].

From the analysis of concretes C1-80, C1-40, and C1-20 it appears that for this type and size of fibre there is no limitation for the use of beams of minor height for the quantification of post-peak parameters. From the results of C2-40, it can be seen that most parameters tend to increase in small beams, especially in group E, however the curves are qualitatively similar. The variability was higher than that found in concretes prepared with F1, this fact could be related to the own characteristics of the fibres.

5. Conclusions

The use of small beams to evaluate the flexural behaviour of steel FRC following the general guidelines of the RILEM TC 162-TDF Recommendation was analysed. Concretes with different content and type of fibres were studied. The main conclusions are summarised as follows.

The general guidelines for the bending test can be applied on smaller beams to obtain the post-peak parameters of FRC. When the fibres length and aggregate maximum size are sufficiently small to be compatible with the dimension of the mould, the use of smaller specimens simplifies the test. The use of small beams can be particularly justified when the specimen dimensions are more representative of the FRC application, considering effects of fibre orientation.

The post-peak parameters (equivalent or residual strengths) do not differ from standard beam considering a significance level of 10%.

When small beams were used there were found some effects in the maximum and first crack strengths especially in concretes incorporating low contents of fibres.

The use of small beams with the same height/span ratio does not modify the relationship between deflection and CMOD. Then, it will also be possible to obtain the post-peak parameters by means of the CMOD response without requiring the measurement of the deflection and avoiding the necessity of using the frame to fix the transducers. In this way the test can be remarkably simplified.

References

[1] Gopalaratnam VS, Gettu R. On the characterization of flexural toughness in fiber reinforced concretes. *Cem Concr Compos* 1995;17:239–54.

[2] Barr B, Gettu R, Al-Oraimi SKA, Bryars LS. Toughness measurement – the need to think again. *Cem Concr Compos* 1996;18(4):281–97.

[3] Gopalaratnam V, Shah S, Batson G, Criswell M, Ramakrishnan V, Wecharatana M. Fracture toughness of fiber reinforced concrete. *ACI Mater J* 1991;88(4):339–53.

[4] Mindess S, Chen L, Morgan DR. Determination of the first-crack strength and flexural toughness of steel fibre-reinforced concrete. *Adv Cem Based Mater*. 1994;1:201–8.

[5] Chen L, Mindess S, Morgan DR, Shah SP, Johnston CD, Pigeon M. Comparative toughness testing of fibre reinforced concrete. In: Stevens et al., editors. *Testing of fibre reinforced concrete ACI SP-155*. Detroit, USA: American Concrete Institute; 1995. p. 41–75.

[6] Trottier JF, Banthia N. Toughness characterization of steel-fiber reinforced concrete. *J Civil Eng Mat, ASCE* 1994;6(2):264–89.

[7] RILEM TC 162-TDF Test and design methods for steel fiber reinforced concrete bending test, final recommendation. *Mat Struc* 2002;35:579–82.

[8] Barragán BE, Gettu R, Martín MA, Zerbino R. Uniaxial tension test for steel fibre reinforced concrete-A parametric study. *Cem Concr Compos* 2003;25(7):767–77.

[9] Barragán B, Gettu R, Agulló L, Zerbino R. Shear failure of steel fiber-reinforced concrete based on push-off tests. *ACI Mater J* 2006;103(4):251–7.

[10] RILEM TC 162-TDF Test and design methods for steel fiber reinforced concrete, σ – ε design method. *Mat Struc* 2003;36:560–7.

[11] Barr BIG, Lee MK. Round-robin analysis of the RILEM TC 162-TDF beam-bending test: Part 1 – test method evaluation. *Mat Struct* 2003;36:609–20.

[12] Barr BIG, Lee MK. Round-robin analysis of the RILEM TC 162-TDF beam-bending test: Part 2 – approximation from the CMOD response. *Mat Struct* 2003;36:621–30.

[13] Barr BIG, Lee MK. Round-robin analysis of the RILEM TC 162-TDF beam-bending test: Part 3 – fibre distribution. *Mat Struct* 2003;36:631–5.

[14] Vandewalle L, Dupont D. Study of the parameters influencing the test results: influence of the width of a beam specimen on the bending test results, BRPR–CT98–08013. *Test Design Methods for Steel Fiber Reinforced Concrete*, sub-task 2.3, Annex 2, in CD, 2002.

[15] Schnütgen B, Erdem E, Steffen SH. Study of the parameters influencing the test results Influence of specimen depth on the toughness parameters, BRPR–CT98–08013. *Test and Design Methods for Steel Fiber Reinforced Concrete*, Sub-task 2.3, Annex 3, in CD, 2002.

[16] Rosenbusch J, Teutsch M. Study of the parameters influencing the test results: Study of the effects of aggregate size and fiber length, BRPR–CT98–08013. *Test and Design Methods for Steel Fiber Reinforced Concrete*, Sub-task 2.3, Annex 4, in CD, 2002.

[17] EN 14651. Test method for metallic fibered concrete – measuring the flexural tensile strength. CEN, Brussels, 2005.

[18] ASTM C-1018. Standard test method for flexural toughness and first-crack strength of fibre-reinforced concrete (using beam with third-point loading), *Annual Book of ASTM Standards*, 04.02, Philadelphia, USA, 1992.

[19] Gettu R, Gardner DR, Saldívar H, Barragán BE. Study of the distribution of orientation of fibers in SFRC specimens. *Mat Struct* 2005;38:31–7.